Heat Mass Transfer (2015) 51:1131–1140
DOI 10.1007/s00231-014-1484-0

ORIGINAL

Dynamic heat and mass transfer modeling and control in carbon dioxide reactive absorption process

Hadi Niknafs · Ahad Ghaemi · Shahrokh Shahhosseini

Received: 21 November 2013 / Accepted: 28 December 2014 / Published online: 8 January 2015

Abstract A dynamic model has been developed for modeling of carbon dioxide reactive absorption. Mass transfers of the species were considered in both directions. The heat and mass transfer differential equations, were solved using the method of lines. The experiments were carried out to evaluate the model perditions, using an absorption pilot plant. A comparison between the experimental data and the simulation results proves the good predictivity of the presented model.

List of symbols

a	Specific packing surface (m^2/m^3)
A	Cross-sectional area (m^2)
C	Molar concentration (mol/m^3)
C_p	Heat capacity ($j/m^3.k$)
CR	Carbonation ratio (–)
E	Specific energy holdup (J/m)
D	Diffusion coefficient (m^2/s)
G	Gas phase molar flow rate (mol/s)
h	Molar enthalpy (J/mol)
ΔH	Heat of reaction (J/mol)
K	Vapor–liquid equilibrium constant (–)
k	Reaction rate constant (lit/mol.s)
k_L	Mass transfer coefficient (m/s)
L	Liquid phase molar flow rate (mol/s)
M	Film conversion parameter (–)
N	Interfacial molar flux ($mol/m^2.s$)
q	Heat flux ($J/m^2.s$)
R	Reaction rate ($mol/m^3.s$)
T	Temperature (K)
x	Liquid phase mole fraction (–)
y	Gas phase mole fraction (–)
Z	Axial co-ordinate (m)

Greek letters

δ	Film thickness (m)
ϕ	Specific molar holdup (mol/m)
φ	Volumetric holdup (m^3/m^3)
λ	Thermal conductivity (W/m.K)

Subscripts

G	Gas phase
L	Liquid phase
i	Component index
j	Segment index
s	Component index

Superscripts

b	Bulk
f	Film
g	Gas
l	Liquid
I	Interface

1 Introduction

Removing toxic gases from exhausted gas streams in chemical and petrochemical industries is a vitally important subject from environmental point of view. Carbon dioxide is one of the main greenhouse gases, which should be removed from atmosphere by means of some common techniques such as reactive absorption, adsorption, membrane separation and microbial CO_2 fixation [1, 2].

H. Niknafs · A. Ghaemi (✉) · S. Shahhosseini
School of Chemical Engineering, Iran University of Science and Technology, P.O. Box 16765-163, Narmak, Tehran, Iran
e-mail: aghaemi@iust.ac.ir

Among all above mentioned methods, the chemical absorption seems to be the most practical and effective technique. Chemical reactions occurring during CO_2 absorption by amines have various advantages regarding the operating conditions such as increasing mass transfer rate and decreasing total operating pressure [2, 3].

Several stage models have been developed for modelling of reactive absorption processes. These models could be classified in two categories: equilibrium and non-equilibrium stage models [4]. In an equilibrium stage model, in each stage, gas and liquid output streams are assumed to be in thermodynamic equilibrium [5]. Due to some unrealistic assumptions in the equilibrium stage models, these models are not appropriate for describing reactive separation processes. Therefore, non-equilibrium models have been developed [6–11]. There are two types of non-equilibrium stage models: mass transfer models and rate-based models. Mass transfer models are based on film theory and are more accurate than equilibrium models. Mostly, in these models enhancement factors are used to calculate the mass transfer rates [6, 7].

Rate-based models include mass and energy balance equations of the two-phases. In these models interactions between the molecules and diffusion phenomena are considered using Maxwell–Stefan equations [10, 11]. Whereas, mass transfer is assumed to be in one direction: gas to liquid phase. However, in the real condition it happens in both directions. In addition, the dynamic predictions of the models are not validated by dynamic experimental data. Therefore in this research a dynamic non-equilibrium model has been developed considering mass transfer in both directions in the gas–liquid interface. In the modeling, a new rigorous correlation has been applied for calculation of carbon dioxide absorption rate [12]. The model has been validated using dynamic experimental data. Also the optimum transfer functions of the reactive absorption of CO_2 variables were obtained for system control of the process.

2 Kinetics and absorption rate of CO_2

Kinetics and reactions of carbon dioxide with ammonia solutions have been extensively presented in the literature [13–16]. Modeling of such reactive system of weak electrolytes requires that carbon dioxide reactions in the carbonated ammonia solutions to be taken into account. The reactions including CO_2 obey first and second order kinetics. Three reactions take place for CO_2; CO_2 and water, CO_2 and amines, and the reaction between CO_2 and hydroxyl ions. CO_2 absorption depends on several items including the amount of CO_2 loading into the liquid solution, chemical reactions tacking place in the liquid phase, CO_2 partial pressure in the gas phase and free ammonia concentration in the solution [12]. The extent of CO_2 loading is often known as carbonation ratio, CR, which is defined as follows [12, 17]:

$$CR = \frac{C_{CO_2}}{C_{NH_3}} = \frac{[CO_2] + [HCO_3^-] + [NH_2COO^-] + [CO_3^{-2}]}{[NH_3] + [NH_2COO^-] + [NH_4^+]} \tag{1}$$

It is clear that carbonation ratio is based on the component concentrations. To express the effects of chemical reactions, film conversion parameter has been introduced. Film conversion parameter indicates the ratio of maximum possible conversion to maximum diffusion transfer rate through the film as follows [12]:

$$M_{CO_2}^2 = \frac{D_{L,CO_2}(k_{NH_3}[NH_3] + k_{OH^-}[OH^-] + k_{H_2O}[H_2O])([CO_2]^* - [CO_2])}{k_{L,CO_2}^2[CO_2]^*} \tag{2}$$

Carbon dioxide mass transfer rate was calculated using correlation based on two dimensionless parameters (CR and M_{CO2}) [12]:

$$N_{CO_2} = CR^{-0.0087} M^{0.894} k_{L,CO_2}([CO_2]^* - [CO_2]) \tag{3}$$

This correlation is more rigorous than other correlations presented in the literature [12]. Moreover, it is applicable for a wide range of operating conditions. In the present process, ammonia and water are transferred from liquid to gas phase. The rate of this transformation for ammonia is calculated using the following equation:

$$N_{NH_3} = -D_{NH_3} \left.\frac{dC_{NH_3}}{dz}\right|_{z=0} \tag{4}$$

where, C_{NH3} is calculated from the following equation [18]:

$$\begin{aligned} C_{NH_3} = {} & \sinh\{[\Phi](z - z^I)\} \sinh^{-1}([\Phi]\delta_L) C_{NH_3^*} \\ & - \sinh\{[\Phi](z - z^I)\} \sinh^{-1}([\Phi]\delta_L) C_{NH_3^e} \end{aligned} \tag{5}$$

where Φ is:

$$[\Phi] = ([D_L]^{-1}[K_L])^{0.5}$$

where D_L is diffusion coefficient in the liquid phase and K_L is reaction rate constant.

3 Mathematical modelling of heat and mass transfer in absorption column

Reactive absorption is a complex rate-controlled process that occurs far from thermodynamic equilibrium. The rate-based model for reactive absorption processes [8, 9, 11] involving the rigorous description of mass and heat transfer phenomena, phase equilibrium relations and chemical

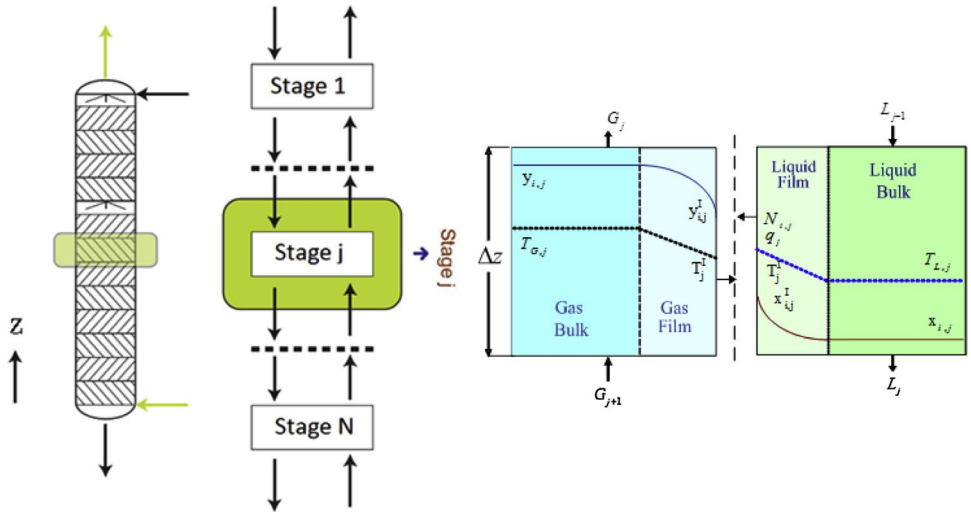

Fig. 1 Stage modeling of reactive absorption column

reactions in both phases is calculated in a number of equivalent stages. Mass transfer is described by the two film model [3], which assumes that mass transfer resistance is limited in the two film regions adjacent to the gas–liquid interface. Gas and liquid bulk phases are in contact only with the corresponding films, while thermodynamic phase equilibrium is assumed to occur only at the interface with no interfacial accumulation. Chemical reactions are considered to take place in both the film of liquid and gas phase [7, 11]. In Fig. 1, the model was described by detail.

The phases in each stage are assumed to be fully mixed because the compositions and temperatures in a particular phase leaving a stage are identical to the bulk phase properties. For simplicity of presentation, only the axial variations of the temperature and components concentration are taken into account, whereas the temperature and components concentration gradients in any cross section of an apparatus are supposed to be negligible. Dynamic differential mass and heat balances with simultaneous calculation of accumulation terms like liquid holdups on each column segment reflect the continuous and dynamic character of the process. In the dynamic component material balances for the liquid bulk phase, changes of both, the specific molar component and the total molar holdup, are considered which thus represent partial differential equations.

$$\frac{\partial\left(x_{i,j}\phi_L\right)}{\partial t} = -\frac{\partial\left(x_{i,j}L_j\right)}{\partial z} + \left(N_{i,j}^{b}a^{I} + R_{i,j}^{lb}\varphi_L\right)A \qquad i = 1,\ldots,n \tag{6}$$

where, ammonia and carbon dioxide total mole fractions are calculated using the following equations:

$$x_{CO_2,j} = x_{[CO_2],j} + x_{[NH_2COO^-],j} + x_{[CO_3^{-2}],j} + x_{[HCO_3^-],j} \tag{7}$$

$$x_{NH_3,j} = x_{[NH_3],j} + x_{[NH_2COO^-],j} + x_{[NH_4^+],j} \tag{8}$$

Mostly, liquid phase in reactive absorption processes is electrolyte solution, so in the multi-component electrolyte systems the following principles should be considered [19]:

(1) Equilibrium of chemical reactions in the solution (dissociation of water and electrolytes and reactions between the electrolytes and/or products of their dissociation) with the deviations from the ideal solution properties being taken into account. (2) Electrolytes Mass balances in the solution. (3) Electroneutrality of the solution [19, 20].

The gas holdup can be neglected due to the low gas phase density at atmospheric operating pressure which leads to the following balance equation for each component of the gas bulk:

$$0 = \frac{\partial\left(G_j y_{i,j}\right)}{\partial z} - \left(N_{i,j}^{b}a^{I}\right)A \qquad i = 1,\ldots,n \tag{9}$$

Mass balance equation for components that transfer from liquid phase to gas phase is:

$$0 = \frac{\partial\left(G_j y_{s,j}\right)}{\partial z} + \left(N_{s,j}^{b}a^{I}\right)A \qquad s = 1,\ldots,m \tag{10}$$

For the determination of axial temperature profiles, differential dynamic heat balances are formulated including the conductive and convective heat fluxes as well as the product of the liquid molar holdup and the specific molar enthalpy:

$$\frac{\partial(C_{p,L}\varphi_L T)}{\partial t} = -\frac{\partial(L_j h_j^{lb})}{\partial z} + (q^{lf}a^{I} + R_j^{lb}\varphi_L\Delta H)A \tag{11}$$

Heat losses were neglected in the enthalpy balance for the liquid bulk phase. The heat flux through the liquid film comprises the conductive and convective terms:

Table 1 Mass transfer coefficients and physical properties

Phase	Parameter	References
Gas	Binary diffusion coefficient	[22]
	Mass transfer coefficient	[21, 23]
	Viscosity	[22]
Liquid	Binary diffusion coefficient	[24]
	Mass transfer coefficient	[22, 23]
	Viscosity	Andrade [22]
	Surface tension	Hakim-Steniberg-stiel [17]

$$q^{gf} = \frac{\lambda^{gf}}{\delta^{gf}}(T^I - T^{gb}) + \sum_{i=1}^{m} N_i^{gf} h_i^{gf} \tag{12}$$

Heat transfer rate to the gas and liquid film interfaces has been given by the following equations, respectively:

$$0 = \frac{\partial(G_j h_j^{gb})}{\partial z} - (q^{gf} a^I)A \tag{13}$$

Heat losses were neglected in the enthalpy balance for the gas bulk. The heat flux through the gas film comprises the conductive and convective terms:

$$q^{lf} = \frac{\lambda^{lf}}{\delta^{lf}}(T^{lb} - T^I) + \sum_{i=1}^{m} N_i^{lf} h_i^{lf} \tag{14}$$

The heat balance for the liquid phase includes the energy holdup as an accumulation term. The energy fluxes across the interface are linked by the continuity equation:

$$q^{gf} - q^{lf} = 0 \tag{15}$$

Summation of mole fractions in each phase equals one. Therefore:

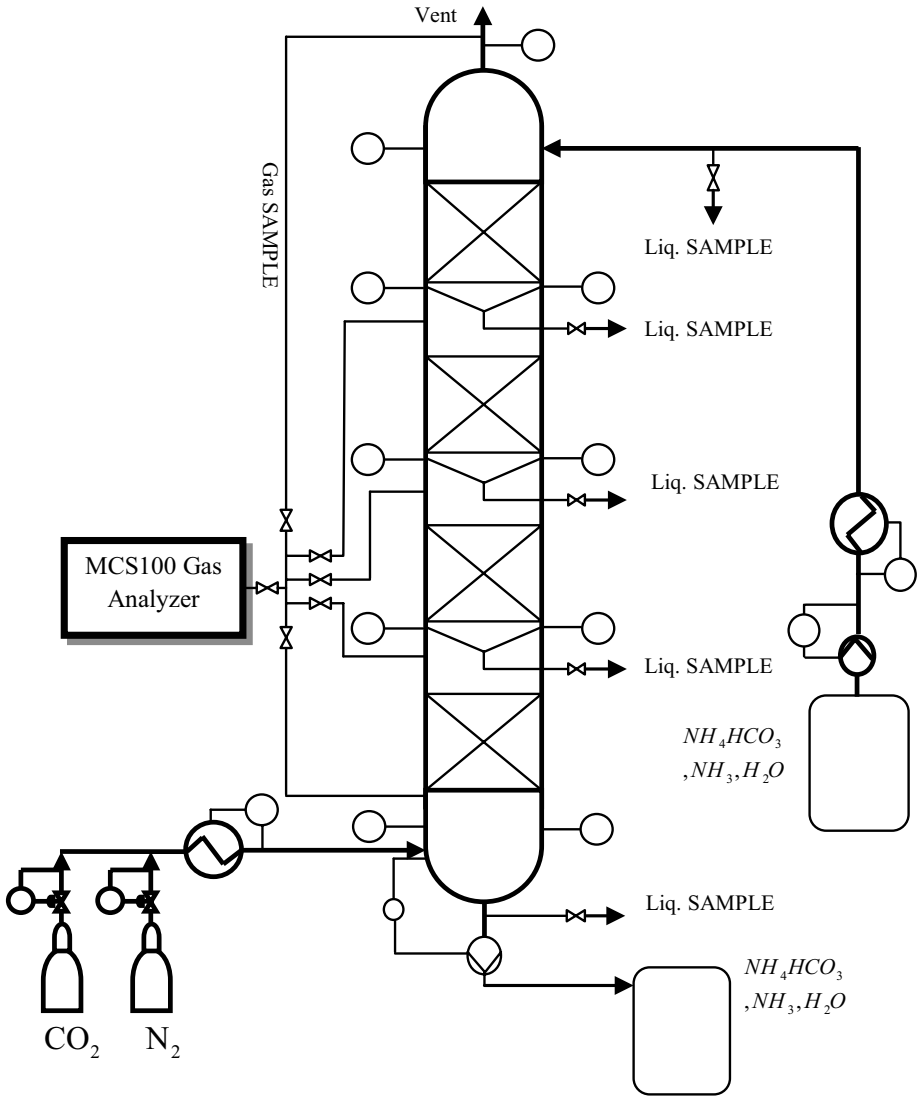

Fig. 2 Schematic of absorption pilot plant

$$\sum_{i=1}^{n} x_i = 1 \tag{16}$$

$$\sum_{i=1}^{n+m} y_i = 1 \tag{17}$$

4 Determination of physical properties and model parameters

Simulation accuracy strongly depends on the values of the parameters related to thermodynamic equilibrium, column hydrodynamic, reaction kinetics and physical properties. The phases are in equilibrium state at the interface. Thus:

$$y_{i,j}^{l} = K_{i,j} x_{i,j}^{l} \quad i = 1, \ldots, n+m \tag{18}$$

where, K is a factor that includes fugacity in the gas phase and activity coefficient in the liquid phase obtained from thermodynamic models. Reactive separation processes occur in the electrolyte solutions. In this study, equilibrium mole fractions of the components at the interface are obtained by Pitzer semi empirical model given by Krop [19]. The presented model parameters are shown in Table 1. Effective diffusion coefficient in the liquid phase is given by Nernst-Hartley, which describes transfer properties in weak electrolyte solutions [21]. Effective diffusion coefficient in the gas phase has been estimated by Wilke-Lee equations for low pressure conditions [22]. The process hydrodynamic influence has been taken into account by applying empirical mass transfer, effective specific area, liquid holdup and pressure drop correlations [21, 23].

Table 2 Input conditions of the absorption column

Process variables	Temp. (k)	NH_3 (mol/h)	N_2 (mol/h)	CO_2 (mol/h)	H_2O (mol/h)
Gas	282.1	0	196.6	90.72	0
Process variables	Temp. (k)	NH_3 (mol/m^3)	CO_2 (mol/m^3)		
Liquid	285.8	500.3	229		

5 Laboratory absorption setup

Figure 2 illustrates the scheme of an absorption column, which has been used to perform the experiments in order to validate the simulation results. This column is made of a glass cylinder with a 105 mm diameter, which contains four packing sections with a height of 650 mm. For redistributing the liquid flow a tray has been put between the sections. Two temperature sensors and two valves were installed on the trays measuring gas and liquid temperature as well as taking samples. The bed packing was made of ceramic Rashing rings (0.5 inch) type.

6 The experimental procedure

The experimental data were taken in dynamic conditions. At the onset of the experiments only nitrogen (the gas phase) was fed at the bottom of the column, CO_2 was added to the gas phase (nitrogen stream) after start up and data was taken after reaching to a distinct flow regime. After about 25 s the system reaches a steady-state condition so there are no changes in the dynamic parameters. The total sampling time was 25 with 3 s sampling interval.

The liquid samples were analyzed using an ion chromatography (IC-762 type from METROHM Company) based on conductivity detection method. The gas samples were analyzed by means of an online gas analyzer MSC100 (from SICKMAIHAK company), which is an extremely compact multi-component infrared photometer for extractive continuous monitoring of flue gases. Operating pressure of the column was atmospheric. The

Table 3 The conditions of the output phases at different times

Time (s)	Gas phase mole fractions (partial pressure/pressure)				T (k)	Liquid phase concentration (mol/m^3)	
	N_2	CO_2	NH_3	H_2O	T_L	Total NH_3	Total CO_2
0	0.684	0.3157	0.0	0.0	285.8	500.3	229.0
3	0.657	0.3084	0.0006	0.034	285.9	500.3	229.3
6	0.662	0.3031	0.0011	0.034	286.2	497.7	235.5
9	0.667	0.2966	0.0021	0.034	286.8	495.1	257.4
12	0.671	0.2919	0.0033	0.034	287.1	492.3	272.9
15	0.674	0.288	0.0042	0.034	288.1	490.2	285.3
18	0.675	0.2857	0.0055	0.034	288.5	486.9	292.0
21	0.679	0.2814	0.0056	0.034	288.9	486.7	306.7
25	0.682	0.2787	0.0057	0.034	289.0	486.5	315.6

conditions of input phases to the absorption column are given in Table 2.

The pilot column results for the phases are demonstrated in Table 3. The mole fraction of water was constant owing to no changes in the gas phase temperature.

7 Numerical solution

All the model equations were partial and ordinary differential equations. These equations were discretized along the column height direction applying the method of lines and finite difference resulting in the coupled ODEs and algebraic equations. The algorithm of the model solution is shown in Fig. 3. All the model equations were numerically solved using the algorithm given in Fig. 3.

8 Control of absorption column

The growing applications of reactive absorption process have necessitated a better understanding of its dynamics and control. In practice, the use of online analyzer to measure the concentrations in a reactive absorption column is unsatisfactory because of its high cost. In addition, the long time delay between taking a sample and obtaining the output of the offline analyzers makes it difficult to be used in a feedback control system. Therefore, determination and use of a transfer function is needed in the control system of a reactive absorption system [25].

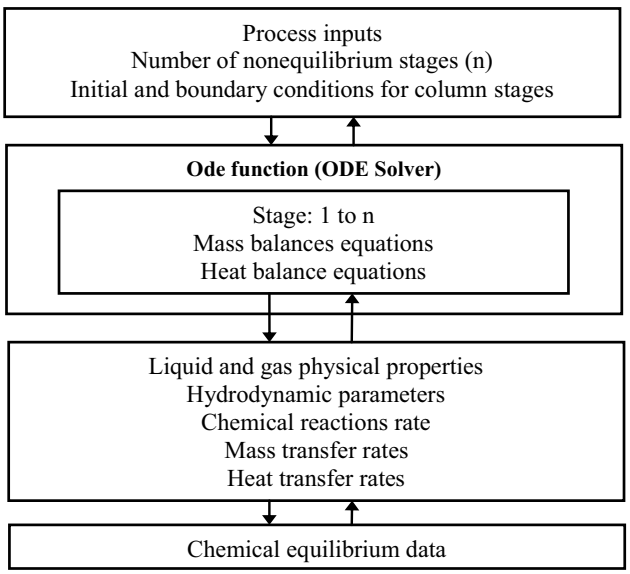

Fig. 3 The algorithm of model equations solution

To design an efficient control strategy, it is necessary to consider the absorption column dynamic behavior. Good prediction of absorption column in different operating conditions depends on driving transfer function of each output variables versus the inputs. A transfer function is calculated by the following equation [26]:

$$H(s) = \frac{Y(s)}{X(s)} = \frac{L\{y(t)\}}{L\{x(t)\}} \tag{19}$$

where, X(s) is an input and Y(s) is a output variable. In the present process, CO_2, N_2 and NH_3 flow rates and liquid phase temperature are the most effective factors influencing on CO_2 absorption.

To achieve the transfer functions, a step change is independently applied to each input variable. CO_2 concentrations are measured at 3 s intervals to accomplish unsteady-state characteristics. Features of applied step changes on each variable and final CO_2 concentration have been listed in Table 4.

Figure 4 shows the variations of CO_2, N_2, NH_3 and temperature in response to the step changes in the input variables. It indicates CO_2 absorption rate responds immediately when N_2 and CO_2 flow step changes start. However, regarding liquid temperature and NH_3 concentration step changes, the rates vary with some delay.

All experimental data of CO_2 concentration due to each variable step change, contributed in development of the transfer functions. The general form of transfer functions, which includes zero, pole, and delay terms, is given in the following equation [27]:

$$H(s) = \frac{K(1 + Tzs)\exp(-Tds)}{(1 + Tp1s)(1 + Tp2s)} \tag{20}$$

In Eq. (19), measured CO_2 concentration and step changes of the input variables have been considered as output and input matrices, respectively. By means of process

Table 4 Characteristics of applied step changes on each variable and final CO_2 concentration

Phase	Variable	Step change	Initial CO2 conc. (mol/m^3)	Final CO2 conc. (mol/m^3)
Gas	N_2	70 to 100 (mol/h)	283.8	299.1
	CO_2	0 to 60 (mol/h)	229.0	315.3
Liquid	T	276.15 to 288.15 (K)	268.0	320.6
	NH_3	478 to 550 (mol/m3)	277.5	392.0

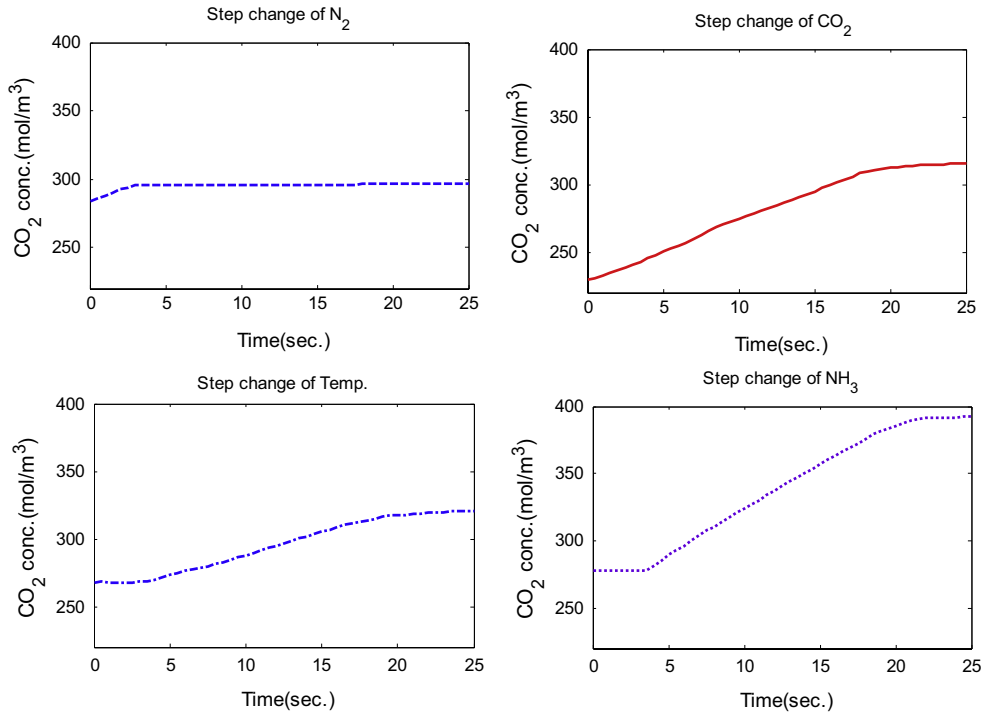

Fig. 4 The changes of output variables for each step changes

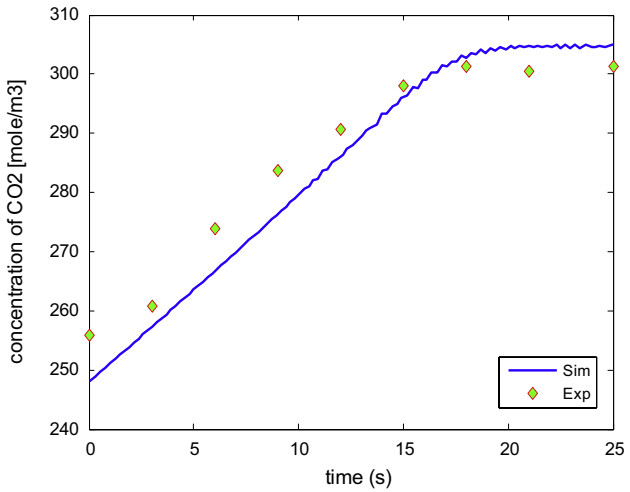

Fig. 5 CO_2 concentration variations with time at the leaving stream

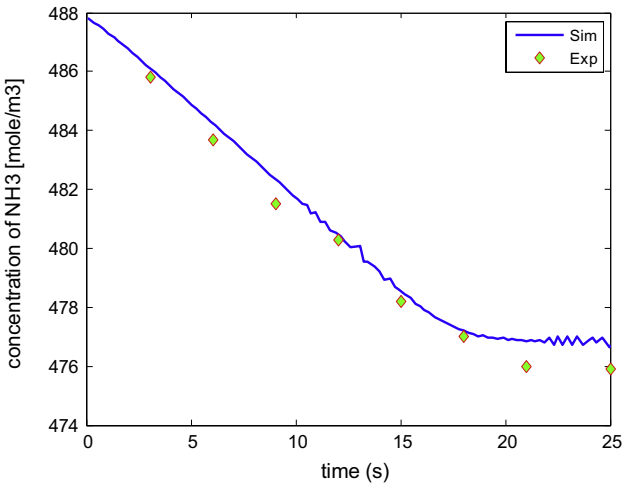

Fig. 6 Ammonia concentration variations at the bottom of the column with time

model the transfer function (Eq. 20) calculation has been done for different cases resulted from the existence and non-existence of the following items: delay term, pole, first and second zero. Estimation of the transfer function started from the simplest functions to more complex ones with a step by step approach. Finally, the simplest function showing the most reasonable prediction is chosen as an optimum transfer function.

9 Results and discussion

Simulations were performed for both dynamic and steady state conditions and the results were validated using dynamic experimental data obtained from the pilot plant. Figure 5 shows the dynamic curve of CO_2 concentration at the bottom of the column. It is clear that there is no change in CO_2 concentration after about 20 s.

Due to transformation of ammonia from the liquid phase to the gas phase, ammonia concentration decreases in the liquid phase. Figure 6 shows the dynamic changes of ammonia concentration in the output of the liquid phase stream.

The reactions of CO_2 in the liquid phase are exothermic, so the liquid temperature increases owing to CO_2 absorption. The packed column loses some heat through its wall, Therefore the experimental data for liquid temperature are lower than the corresponding predictions of the model.

Figure 7 indicates the liquid temperature rises at the output of the liquid stream and reaches to a constant amount at the steady-state condition.

Table 5 shows the experimental and simulation results of the process. The data and the simulation results have been compared using relative deviation relation as follows:

$$RD\,\% = \frac{\left|X_{Exp.} - X_{Cal.}\right|}{X_{Exp.}} \times 100 \tag{21}$$

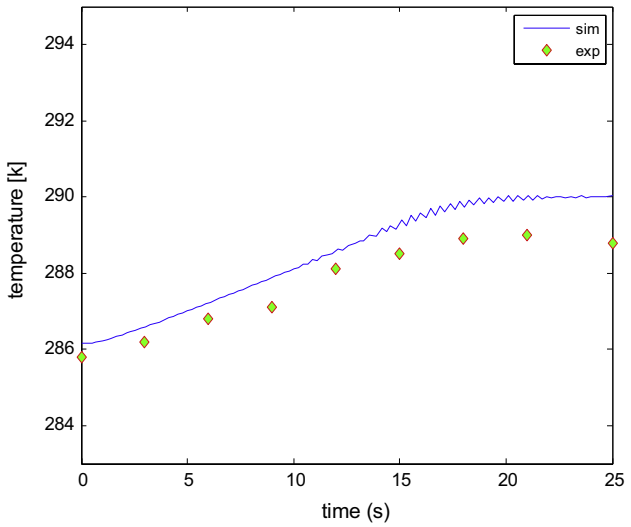

Fig. 7 Liquid temperatures at the bottom of the column versus time

The comparison revealed there is a good agreement between the model predictions and the data. The model was validated using different experimental data which occurred at different operation conditions. Table 5 shows a 0.5 % minimum deviation and a 2.5 % maximum deviation between simulation results and the data for CO_2 concentration in the liquid phase.

The step change results in liquid temperature are shown in Figs. 8 and 9. In Fig. 8, liquid temperature reaches to steady state after about 25 s. Liquid temperature was increased 2° from 25 to 30 s. It shows that after about 50 s, the temperature change arrives to the bottom of the column.

In the second step change, after 25 s, liquid temperature at the top of absorption column is increased by 2°. In Fig. 9, temperature changes in all stages are displayed. This figure shows the model remains stabile after the step changes.

The transfer function parameters were calculated in different conditions using the process model. For instance, transfer function parameters for 12 °C step-changes in solution temperature are listed in Table 6. As shown in this table, the P_1Z function is the simplest one, with an acceptable CO_2 concentration prediction affected by solution temperature step changes. Therefore, P_1Z function has been chosen as the optimum transfer function for this case. In Fig. 10 transfer functions of carbon dioxide concentration were presented using the process model.

Putting the constants values in Eq. (19) results in following equation:

$$F(s) = \frac{1.12\exp(-14.7s)}{(1 + 4.05s)} \tag{22}$$

It is clear from above equation that the transfer function consist of a delay term resulted from the time, which liquid phase needs to pass from top of the column to the sampling point (bottom of the column). The same calculation was carried out for three other variables (CO_2, N_2 and NH_3). Flow rate step changes and the optimum transfer function were determined as well. The results are indicated in

Table 5 Comparison of the dynamic experimental and simulation results

Time[s]	$CO_{2,Sim}$ (mol/m^3)	$CO_{2,Exp}$ (mol/m^3)	RD %	$NH_{3,Sim}$ (mol/m^3)	$NH_{3,Exp}$ (mol/m^3)	RD %	T_{Sim} (k)	T_{Exp} (k)	RD %
0	255.8	255.8	0.00	488.0	487.5	0.10	286.2	285.8	0.14
3	257.4	260.8	1.30	486.1	485.8	0.06	286.6	286.2	0.14
6	267.0	273.8	2.48	484.2	483.7	0.10	287.2	286.8	0.14
9	276.9	283.7	2.40	482.2	481.5	0.15	287.8	287.1	0.24
12	286.4	290.6	1.45	480.5	480.3	0.04	288.7	288.1	0.21
15	296.0	298.1	0.70	478.6	478.2	0.08	289.0	288.5	0.17
18	302.7	301.2	0.49	477.2	477.0	0.04	289.7	288.9	0.28
21	304.7	300.4	1.43	476.9	476.0	0.19	289.6	289.0	0.21
25	305.1	301.3	1.26	476.7	475.9	0.17	289.6	288.8	0.28

Table 6. Function accuracy to predict the process, computation time and function simplicity were optimized to select of these functions.

According to Table 7, transfer functions of both solution temperature and NH_3 concentration step changes include the delay term. In addition, Fig. 6 shows a sharper slop for NH_3 curve compared to temperature curve. Regarding the transfer functions, it was already expected that NH_3 gain should be greater than temperature gain. This was proved by comparing the equations of these two variables. In conclusion, the most important result of this study is: Transfer function of liquid phase variables can be modeled with delay term due to the time needed for the liquid to pass along the column. On the other hand, the first and second order functions predict an acceptable absorption rate in gas phase without regard to the delay term due to gas phase injection at the sampling point.

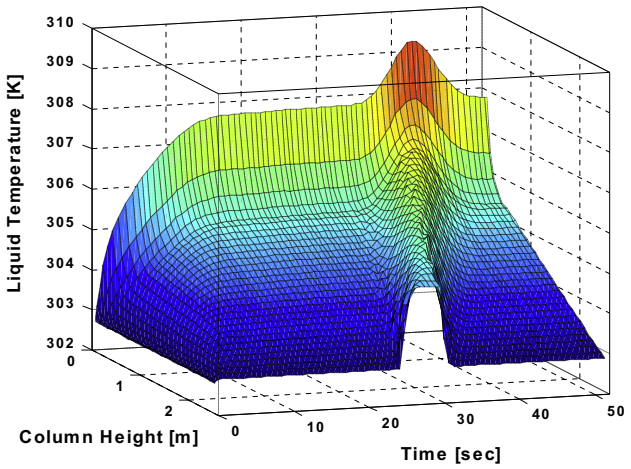

Fig. 8 Liquid temperature after a step change (2 °C) between time 25 and 30 s

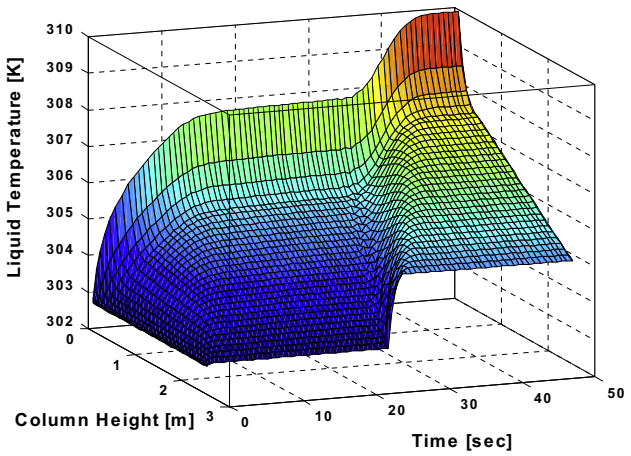

Fig. 9 A step change 2 °C in liquid phase between time 25 and 50 s

10 Conclusions

In this work, a nonequilibrium dynamic model was developed for reactive absorption of carbon dioxide into chemical solutions. A rigorous correlation based on film conversion parameter and carbonation ratio was used in this

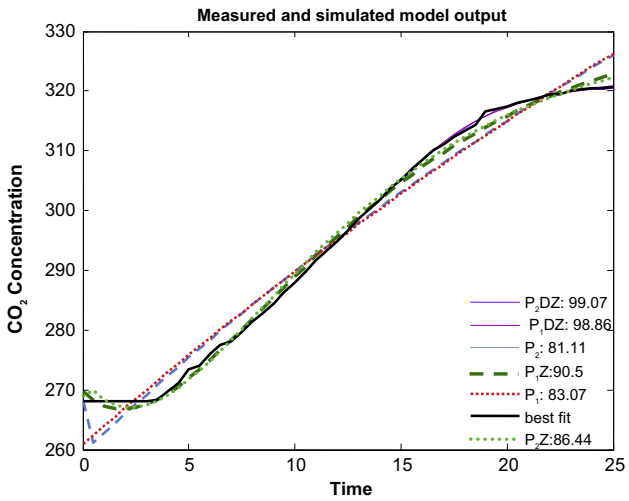

Fig. 10 Transfer function approximations for candidate functions

Table 7 Optimum transfer function for each variables step change

Variable	N_2	CO_2	T	NH_3
Transfer function	$\frac{2.96(1+0.388s)}{(1+1.4s)}$	$\frac{6.19}{(1+2.07s)}$	$\frac{1.12\exp(-14.7s)}{(1+4.05s)}$	$\frac{1.72\exp(-14.79s)}{(1+3.86s)}$

Table 6 Parameters of transfer function in various candidate functions

	P_1	P_2	P_1Z	P_2Z	P1DZ	P_2D
K	1.6785	1.1547	1.5248	1.1441	1.1189	1.1137
Tp_1	71.905	6.7066	54.173	6.6051	4.0477	1.9693
Tp_2	–	6.86	–	5.7893	–	1.9687
Td	–	–	–	–	14.7	15
Tz	–	–	−24.382	−16.028	–	–
Error (%)	83.07	81.11	90.5	86.44	98.86	99.07

model in order to calculate carbon dioxide absorption rate. The model equations were solved simultaneously using rigorous and stable method of lines. The mass transfer experiments were conducted using the absorption pilot plant. The dynamic simulation result was evaluated using dynamic experimental data showing maximum 2.5 % deviation for carbon dioxide concentration in the liquid phase. The results of step changes in temperature showed that the dynamic model is stable within the operating range of the variations. The optimum transfer function for absorption parameters can be used for control of the process.

References

1. Kohl A, Nielsen R (1997) Gas purification, 5th edn. Gulf Publishing Company, Houston
2. Danckwerts PV (1970) Gas-liquid reactions. McGraw-Hill, New York
3. Taylor R, Krishna R (1993) Multicomponent mass transfer. Wiley, New York
4. Stankiewicz A, Moulijn J (2004) Re-engineering the chemical processing plant. Marcel Dekker Inc, New York
5. Sorel E (1893) La rectification de lalcool. Gauthiers-Villaisetfils, Paris
6. Bradley KJ, Andre H (1972) A dynamic analysis of a packed gas absorber. Can J Chem Eng 50:528–533
7. Brettschneider O, Thiele R, Faber R, Thielert H, Wozny G (2004) Experimental investigation and simulation of the chemical absorption in a packed column for the system NH_3–CO_2–H_2S–NaOH–H_2O. Sep Purif Technol 39:139–159
8. Kenig EY, Wiesner U, Groak A (1997) Modeling of reactive absorption using the Maxwell Stefan equation. Ind Eng Chem Res 36:4325–4334
9. Kenig EY, Schneider R, Gorak A (1999) Rigorous dynamic modelling of complex reactive absorption processes. Chem Eng Sci 54:5195–5203
10. Kenig EY, Kucka L, Gorak A (2003) Rigorous modeling of reactive absorption processes. Chem Eng Technol 26:631–646
11. Ghaemi A, Shahhosseini Sh, Ghannadi Maragheh M (2009) Non-equilibrium modeling of reactive absorption processes. Chem Eng Commun 196:1076–1089
12. Ghaemi A, Torab-Mostaedi M, Ghannadi Maragheh M (2011) Kinetics and absorption rate of CO_2 into partially carbonated ammonia solutions. Chem Eng Commun 198:1169–1181
13. Aboudheir A, Tontiwachwuthikul P, Chakma A, Idem R (2003) Kinetics of reactive absorption of carbon dioxide in high CO2-loaded, concentrated aqueous MEA solutions. Chem Eng Sci 58:5195–5210
14. Yeh AC, Hsunling B (1999) Comparison of ammonia and monoethanolamine solvents to reduce CO_2 greenhouse gas emissions. Sci Total Environ 228:121–133
15. Navaza JM, Gomez D, Dolores M, Rubia L (2009) Removal process of CO_2 using MDEA aqueous solutions in a bubble column reactor. Chem Eng J 146:184–188
16. Rangawala HA, Morrell BR, Mather AE, Otto FD (1992) Absorption of CO_2 into aqueous tertiary amine/MEA solutions. Can J Chem Eng 70:482–490
17. Shen J, Yang Y, Maa J (1999) Promotion mechanism for CO_2 absorption into partially carbonated NH_3 solutions. J Chem Eng Jpn 32:378–381
18. Kenig EY, Schneider R, Gorak A (2001) Multicomponent unsteady-state film model: a general analytical solution to the linearized diffusion–reaction problem. Chem Eng J 83:85–94
19. Krop J (1999) New approach to simplify the equation for the excess gibbs free energy of aqueous solution of electrolytes applied to the modeling of the NH_3–CO_2–H_2O vapor–liquid equilibria. J Fluid Ph Equilib 163:209–229
20. Zemaitis J, Clark DM, Scrivner NC (1986) Handbook of aqueous electrolyte thermodynamics. AIChE, New York
21. Billet R, Schultes M (1993) Predicting mass transfer in packed columns. Chem Eng Technol 16:1–9
22. Reid R, Prausnits J, Poling B (1987) The properties of gases and liquids. McGraw-Hill, New York
23. Onda K, Takeuch H, Okumoto Y (1968) Transfer coefficient between gas and liquid phase in packed columns. J Eng Jpn 1:56–62
24. Siddiqi M, Lucas K (1986) Correlations for prediction of diffusion in liquids. Can J Chem Eng 64:839–843
25. Olanrewaju MJ, Al-Arfaj MA (2005) Development and application of linear process model in estimation and control of reactive distillation. Comput Chem Eng 30:147–157
26. Coughanowr DR, Koppel LB (1965) Process systems analysis and control. McGraw-Hill, New York
27. Stephanopoulos G (1984) Chemical process control an introduction to theory and practice. Prentice Hall, Englewood Cliffs, New Jersey